UNIVERSITY JOSEPH FOURIER
LABORATORY TIMC-IMAG

Biomechanical 3D simulation of the invagination process

Athanasios Lontos

Master of Science Thesis

Grenoble, July 2010

UNIVERSITY JOSEPH FOURIER
LABORATORY TIMC-IMAG

Biomechanical 3D simulation of the invagination process

A thesis submitted by

Athanasios Lontos

in partial fulfillment for the

Master of Science Degree

Author:

Athanasios Lontos

Commitee:

Emmanuel Promayon, Assistant Professor
University Joseph Fourier
Supervisor

Jacques Demongeot, Director of the TIMC-IMAG laboratory
TIMC-IMAG laboratory
Supervisor

Oded Maler, Research Director CNRS-VERIMAG
Member

July 2010

Biomechanical 3D simulation of the invagination process

Athanasios Lontos

Master of Science Thesis

Abstract

The process of gastrulation is an important early stage of morphogenesis. It is a very complex procedure, during which the organs of the foetus take their initial shape. It is controled by genetic, chemical and mechanical factors, but the contribution of each one of them to the procedure, is still unknown.

Invagination is the initial step of gastrulation. During this procedure, the cells are guided by chemotaxy, in order to supply their energy demand. It has been observed that some cells start to take the shape of a bottle (bottle-cells), decreasing their surface close to the nourishment fluid. As a result of their surface reduction, the neighboring cells are pulled toward the bottle cells. This results to the blastula performing an inner folding and finally "surrounding" the nourishment.

The movement of cells during gastrulation is gravely affected by the centriole, the cadherins and the myosin fibers. They are inner-cell structures composed by proteins. The understanding of the effect of these factors on cell beavior, is a crucial step towards explaining the entire procedure of morphogenesis.

We propose in this work an approach of the phenomenon of invagination based exclusively on the laws of physics and mechanics. For this purpose, we have created a three-dimensional model and attempted to simulate the initiation of the procedure of invagination. The results of our experiments show that in-vivo cell behavior is adequately simulated and that this approach can be enhanced in order to simulate other genetic processes as well.

Supervisors

Emmanuel Promayon

Assistant Professor

Engineering School of Information Technology for Heath

University Joseph Fourier

Jacques Demongeot

Director of TIMC-IMAG

Τρισδιαστατη προσομοιωση της διαδικασιας της εγκολπωσης

Αθανασιος Λοντος

Μεταπτυχιακη εργασια

Η γαστριδιωση ειναι ενα πολυ σημαντικο πρωιμο σταδιο της μορφογενεσης. Ειναι μια πολυπλοκη διαδικασια, κατα την οποια τα εμβρυικα οργανα λαμβανουν την αρχικη τους μορφη. Ελεγχεται απο γενετικους, χημικους και φυσικους παραγοντες, ομως η συμβολη του καθε παραγοντα δεν ειναι ακομα πληρως γνωστη.

Το αρχικο σταδιο της γαστριδιωσης ειναι η εγκολπωση. Κατα τη διαρκεια αυτης της διαδικασιας, τα κυτταρα καθοδηγουνται απο παραγοντες χημιοταξιας, ωστε να ικανοποιησουντις ενεργειακες τους απαιτησεις. Εχει παρατηρηθει οτι καποια κυτταρα λαμβανουν το σχημα μπουκαλιου, μειωνοντας την επιφανεια τους που βρισκεται πιο κοντα στην τροφη. Ως αποτελεσμα, τα γειτονικα κυτταρα ελκονται προς τα κυτταρα με σχημα μπουκαλιου. Κατα συνεπεια, ο βλαστος (εμβρυο) δημιουργει μια εσωτερικη αναδιπλωση προκειμενου να 'περικυκλωσει' την τροφη.

Η κινηση των κυτταρων κατα τη διαρκεια της γαστριδιωσης επηρρεαζεται σε μεγαλο βαθμο απο το 'κεντροσωμα', τους δεσμους κυτταρου-κυτταρου και τις ινες μυοσινης. Ειναι ενδοκυτταρικες δομες αποτελουμενες απο πρωτεινες. Η καταννοηση της επιρροης αυτων των παραγοντων στην κυτταρικη συμπεριφορα ειναι ενα κρισιμο βημα προς την εξηγηση ολοκληρης της διαδικασιας της μορφογενεσης.

Στο πλαισιο της συγκεκριμενης εργασιας προτεινεται μια προσεγγιση του φαινομενου της εγκολπωσης βασισμενη εξολοκληρου στους νομους της φυσικης και της μηχανικης. Γι΄ αυτο το σκοπο, δημιουργησα ενα μοντελο τριων διαστασεων και προσπαθησα να προσομοιωσω την εκκινηση της διαδικασιας της εγκολπωσης. Τα αποτελεσματα των πειραματων μας δειχνουν οτι η πραγματικη κυτταρικη συμπεριφορα προσομοιωνεται ικανοποιητικα και αυτη η προσεγγιση μπορει να επαυξηθει προκειμενου να προσομοιωθουν και αλλες γενετικες λειτουργιες.

Εποπτες

Emmanuel Promayon

Maître de Conférences

Équipe GMCAO

Laboratoire TIMC-IMAG

Jacques Demongeot

Directeur du Laboratoire TIMC-IMAG

Laboratoire TIMC-IMAG

Simulation 3D biomécanique du processus d' invagination

Athanasios Lontos

Projet du Master

Le processus d' invagination est une étape très importante de la morphogenèse. C' est un processus très compliqué, qui décrit l' initiation de la formation des organes du foetus. Il est controlé par des facteurs génétiques, chimiques et mécaniques, dont on ne connait pas exactement la contribution.

L' invagination est la première étape de la gastrulation. Pendant ce processus, les cellules sont guidées par chimiotaxie, pour satisfaire leur demande d' energie. Des expériences scientifiques montrent que quelques cellules commencent à se déformer en prennant la forme d' une bouteille (bottle-cells). Par conséquant, leur surface la plus proche à la nourriture decroît, attirant les cellules voisines et donnant lieu à l' initiation de l' invagination, i.e. le plissement vers l ' intérieur.

Le mouvement des cellules pendant la gastrulation est particulièrement affecté par le centriole, les cadherines et le cytosquelette, structures situées dans la cellule composées par des protéines. La compréhension de l' effet de chacun de ces facteurs sur le comportement des cellules est décisif pour expliquer le processus entier de la morphogenèse.

Dans ce travail, nous proposons une approche du phénomène d' invagination basée uniquement sur les lois de la physique, de la mécanique et de la géométrie. Dans ce but, nous avons créé un model tri-dimensionel pour simuler l' initiation du processus de l' invagination. Les résultats de notre expérimentation montrent que le comportement in-vivo des cellules est convenablement simulé et que cette approche peut être renforcée pour modeliser d' autres processus génétiques.

Superviseurs

Emmanuel Promayon

Maître de Conférences

Équipe GMCAO

Laboratoire TIMC-IMAG

Jacques Demongeot

Directeur du Laboratoire TIMC-IMAG

Laboratoire TIMC-IMAG

Acknowledgements

I am extremely grateful to my supervisor, Emmanuel Promayon, for giving me the opportunity to work on the field of 3D Modelling and Simulating Morphogenesis and for our very productive cooperation. Without his guidance and support this project would never have been realized.

In addition, I would like to thank Jacques Demongeot for his valuable help and advice during my research work. His inspiration and contribution in the biological aspect of our research work were crucial in order for the project to be complete.

I would also like to thank the team coordinator, Jocelyne Troccaz, for the creation of such a hospitable and work-friendly environment among the members of the GMCAO team.

A "grand merci" to all the members of the GMCAO team, stagiaires, MSc students, PhD students, post-docs and research staff for their kindness and hospitality. Working with them was a great experience for me.

I would like to thank professors Vassilis Christophides and Saddek Bensalem, the coordinators of the Greek-french postgraduate studies program in Heraklion and Grenoble respectively, for their valuable advice.

Finally, I would like to express my gratitude to my family and friends from Greece, who supported my decision to come to Grenoble for my master project and have always been there for me, whenever and wherever I needed them.

Laboratory TIMC-IMAG

The laboratory TIMC-IMAG (Techniques de l' Ingénierie Médicale et de la Complexité - Informatique, Mathématiques et Applications de Grenoble) gathers scientists and clinicians towards the use of computer science and applied mathematics for understanding and controlling normal and pathological processes in biology and healthcare. This multi-disciplinary activity both contributes to the basic knowledge of those domains and to the development of systems for computer-assisted diagnosis and therapy.

Team GMCAO

The ultimate objective of the GMCAO (Gestes Médico-Chirurgicaux Assistés par Ordinateur) research group is clinical: the purpose is to assist the physician or surgeon in the successful execution of diagnostic or therapeutic gestures by minimizing invasiveness whilst improving accuracy. This general objective involves the quantitative processing of multi-modal patient data and medical knowledge, the fusion of all those information, the planning of an optimal strategy for diagnosis and therapy and the ability to transfer safely and accurately this plan to the operative conditions. This last stage is performed through navigational or robotic assistance. Simulation may also assist the planning phase or the educational part of surgery. This general framework results in multi-disciplinary research, technological development, clinical evaluation and industrial dissemination. The GMCAO group activity follows those lines.

Contents

List of Figures

List of Tables

Chapter 1

Introduction

1.1 Introduction

Morphogenesis is a general concept in biology including all the processes which generate shapes and cellular organizations in a living organism. It originates from the combination of two greek words, "$\mu o \varrho \varphi \eta$" ("morphe", which stands for form, shape) and "$\gamma \epsilon \nu \epsilon \sigma \iota \varsigma$" ("genesis" which stands for principle, origin, birth). Consequently, we would say that morphogenesis means "Birth of forms". This vague meaning has promulgated it to be a very famous term, when examining the factors and parameters controling the creation of tissues, organs and ultimately life.

In general, we could say that there are three levels of control participating in all the cell activities: genetic, chemical and mechanical. The questions that gave birth to this master thesis are: "Up to which point these procedures are controlled by the rules of genetics" and "Is it possible to describe and simulate the generation of shape and cellular/tissue organisation using a model that obeys solely to the laws of mechanics and physics?". In order to be approved, or rejected, this assumption needs a vast amount of experimenting, modeling and simulating, for which, a small contribution, is being described here.

A very important stage of morphogenesis is gastrulation. It is an early stage, including mass movement of cells to form complex structures (e.g. tissues) from a simple starting form. Experiments in vivo have shown that there are many types of mass cell movement taking place during gastrulation: ingression, invagination, involution, epiboly, intercalation and convergent extension. In the course of this paper, we focus on the simulation of the phenomenon of invagination of cells.

As the process of gastrulation varies from one organism to another, for the purpose of our experiment, we have chosen a very typical insect, Drosophila melanogaster, one of the most

commonly used model organisms in biology, including studies in genetics, physiology, microbial pathogenesis and life history evolution. Invagination is an early procedure of gastrulation, which initiates shape formation for the organs of the Drosophila melanogaster.

As far as the behavior of cells participating in our simulation model is concerned, we have adopted the basic principles presented in [FD08] and [ADG09]. The structure of cells used for our experiments is based on the work of [MKW08] and [FD08]. It is a tubular structure formed by a group of cells. During the process of invagination, the cells of this structure are guided by chemotaxy, in order to supply their energy demand. Although the details of the process are yet unclear, research has shown that some cells start to take the shape of a bottle, decreasing their exchange surface with the nourishment fluid ([HK88]). This results to the formation of a curve, directed to the inner part of the structure. As a result of their surface reduction, the neighboring cells are pulled toward the bottle cells increasing the invagination.

The cell contraction is due to myosine fibers located on the edge of the cell ([DHPC$^+$05]). These are thin filaments found on the cytoplasm of the cytoskeleton of all the eukaryotic cells. They are flexible, versatile and relatively strong and they serve as tensile platforms for myosin's ATP hydrolysis-dependent pulling action in muscle contraction and uropod advancement.

1.2 Contribution

The main contribution of this thesis lies in providing proof that mechanics inflicts a much greater effect on cell behavior than the one attributed to it, so far. The key difference to prior models based on mechanics, is that, while most authors rely on differential equations in order to simulate the behavior of cells, we focus on the geometry of the blastula. We attempt to explain the massive cell movements taking place during the procedure of invagination, by modelling the effects of all chemical and biological factors, as forces applied on the particles defining the geometry of the structure.

An additional contribution lies on the monitoring of certain factors which affect the procedure of invagination. Consequently, we monitor the displacement of the centrioles of the cells, the sum of forces applied on them and the $surface/volume$ ratio for each individual cell. We then try to compare them with the results deriving from in vivo experiments and explain the variations between the experiments and our simulation. Finally, we propose specific enhancements and alternative approaches regarding the modeling of the chemical and biological factors affecting our simulation, in order to cover all possible aspects of the procedure of invagination.

1.3 Thesis Organization

The remainder of this thesis is organized as follows. In chapter 2, we present the biomechanical model we used during this thesis. We analyze the structural details of the model and the way we included the effects of the chemical and genetic factors. In chapter 3, we describe the process of the simulation and its results. In chapter 4, we refer extensively to the algorithms, software and methods we relied on during this work. Finally, Chapter 5 concludes the thesis and suggests insights, alternative approaches and further work to be done in order for the model to be enhanced.

Chapter 2

Physical model of invagination in Drosophila melanogaster

2.1 Structure of the proposed model

Several successful models have already been created in order to simulate the procedure of invagination in the drosophila melanogaster. Although it has been extensively monitored, the parameters driving the movement and deformation of cells, are not fully explained. In the next paragraphs we are going to describe the structure of our physical model, the parameters we used to create it, the assumptions we made and the new possibilities and questions raised by this approach.

TABLE 2.1: **Cell Modeling**

Cell in vivo	**Proposed Model**
Cell	Hexahedral cellular object composed by 9 particles
Cell formation during the process of invagination	Structure formed by a flat area of 8 cell columns and a curved area of 7 cell columns
Orthogonal perpendicular myosine fibers	Active fibers connecting the 4 top particles of the cellular object
Centriole	Center particle
Cadherins	Common particles on the "touching" sides of the cells
Cell shape deformation	Incompressibility, elasticity and contractility properties

This table presents the biological aspects incuded in our model and the corresponding modeling concept used for the simulation.

This work is dedicated to examining the area of the structure where the phenomenon begins. As a result, we have modeled the upper part of one side of the tube of cells (Figure 2.1) as described in [ADG09]. In our approach, the structure consists of 75 cells arranged in 15 columns of 5 cells each. The first 8 columns form the flat part of the structure. The curvature of the structure starts at column 9 and ends at column 15, for a total curvature of 90° (Figure 2.2(a)).

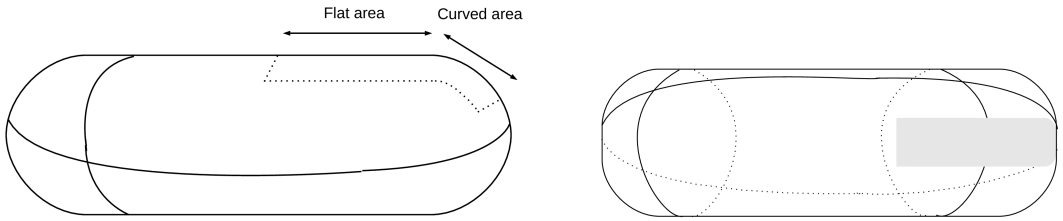

(a) (b)

FIGURE 2.1: **Representation of the modeled area.** (a) The modeled area of the tube defined by the doted line, as seen from a side point of view. The structure is divided into two sub-areas, the flat and the curved. (b) The modeled area of the tube, defined by the grey area, as seen from a top point of view.

Each cell is modeled as a hexahedral object, composed by 9 particles and 6 facets. 8 particles are used as the vertices of the hexaedron and one particle is located in the middle, denoting the centriole of each cell. The cells, with the aid of a biomechanical library, are defined as individual physical objects, with three distinct characteristics: incompressibility, elasticity and contractility. The relation between the biological and in-silico cells is presented in Table 2.1.

The particles are modeled as nodes with physical attributes and the ability to interact with their environment. They are defined by their position and their mass. Elastic and muscular forces are applied on them and they can also be submited to boundary conditions. Their combined displacement is the crucial factor that affects the cell deformation and movement.

The incompressibility algorithm, uses the facets' geometry and a displacement constraint, in order to keep the volume of cells constant. Elasticity forces are defined between neighboring particles in order to model the tissue reaction against deformation. The elasticity parameters have a small value, so that the cell shapes can be modified quite easily by other forces. As a result, we have deformable cells, with nearly unchangeable volumes (which imitates the behavior of cells in vivo). In addition, using muscular forces, we can force the cellular objects to contract

according to the demands of our experiment (contractility property). The implementing of these properties is described extensively in the Materials and Methods section of this work.

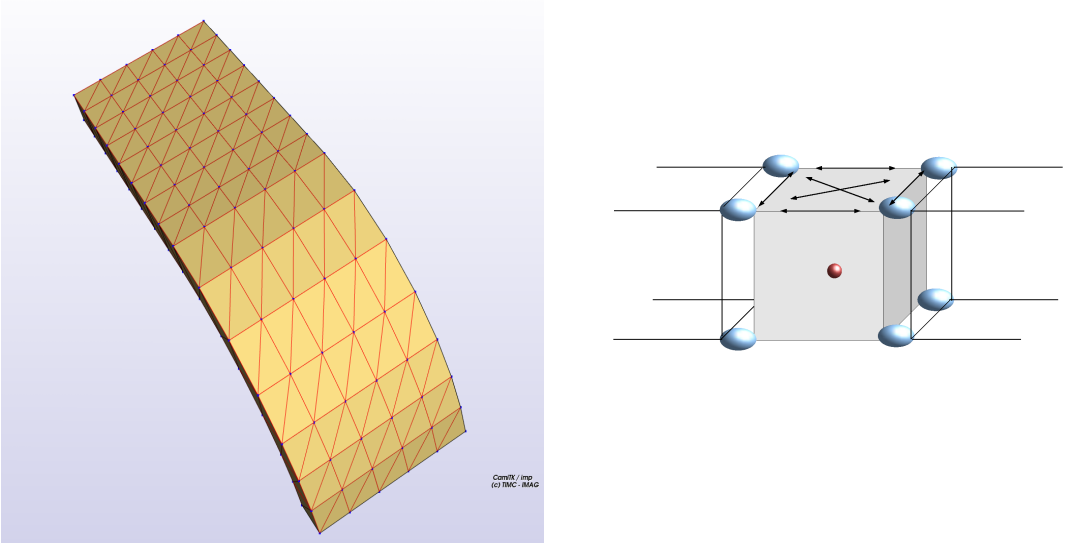

(a) (b)

FIGURE 2.2: **Representation of the structure at its initial form and of the forces imposed on the particles of the top facet of the cells.** (a) The flat area consists of 8 columns of 5 cells each and the curved area consists of 7 columns of 5 cells each, forming a total curvature of 90°. (b) 3D representation of the muscular forces applied on the atoms located on the top facet of the cells in the middle row. The atom pointed in a red sphere represents the centriole. At the beginning of the simulation, it is located in the center of the cell, but as the simulation advances, it moves downward, following the movement of the cell.

2.2 Modeling inner-cell structures

In vivo experiments have shown that neighboring cells form protein-based cell adhesion molecules, resulting to firm connection between each other ([ASK98] and [Tak91]). These protein molecules are called cadherins (Calcium-dependent adhesion molecules) and they are a class of type-1 transmembrane proteins. As there are numerous cadherins formed on the touching surfaces of cells, the forces created and applied by them, are scattered throughout their whole envelope. In our model, we have considered cadherins to offer very strong linking between cells. Therefore, the vertices of the hexahedron are merged, summing up the forces and constraints of all concurrently surrounding cells (2.3(a)). This allows a faster propagation of the forces during the simulation.

The top atoms of each cell of the middle row are linked by muscular forces, which are used to model the forces applied by the orthogonal perpendicular myosine fibers (table 2.1), as shown on Figure 2.2(b).

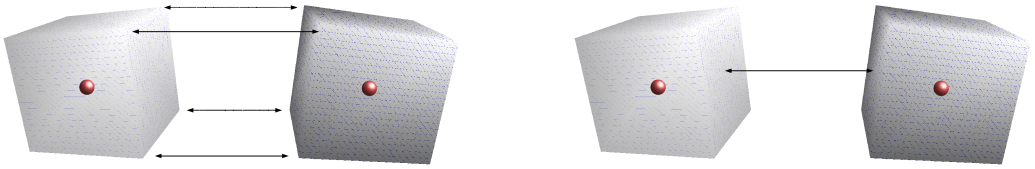

(a) (b)

FIGURE 2.3: **Representation of the cell-cell bonds in our simulation** (a) The cells form liaisons with each other with the aid of protein adhesion molecules called cadherins. In our simulation we have assumed that they can be represented by common atoms located on the vertices of the touching sides of neighboring cells, as proposed by [DCEM09] (b) Proposing an approach where the modeled cadherins are located on the isobarycenter of the touching facets of the neighbouring cells

2.3 Boundary Conditions

In order to verify the symmetry of the simulation, we have applied boundary conditions to the movement of some particles. (Figure 2.4):

- The first boundary condition implies that the edges of the structure cannot move in any direction (Figures 2.4(a) and 2.4(b)).
- The second boundary condition is applied on the side parts of the structure (Figures 2.4(c) and 2.4(d). These atoms can "slide" on the x and y axis but they cannot move on the z axis.

These boundary conditions allow the simulation to consider that this model is a part of a bigger structure, with cells expanding from all sides, in order to form a tubular shape, as presented in Figure 2.1.

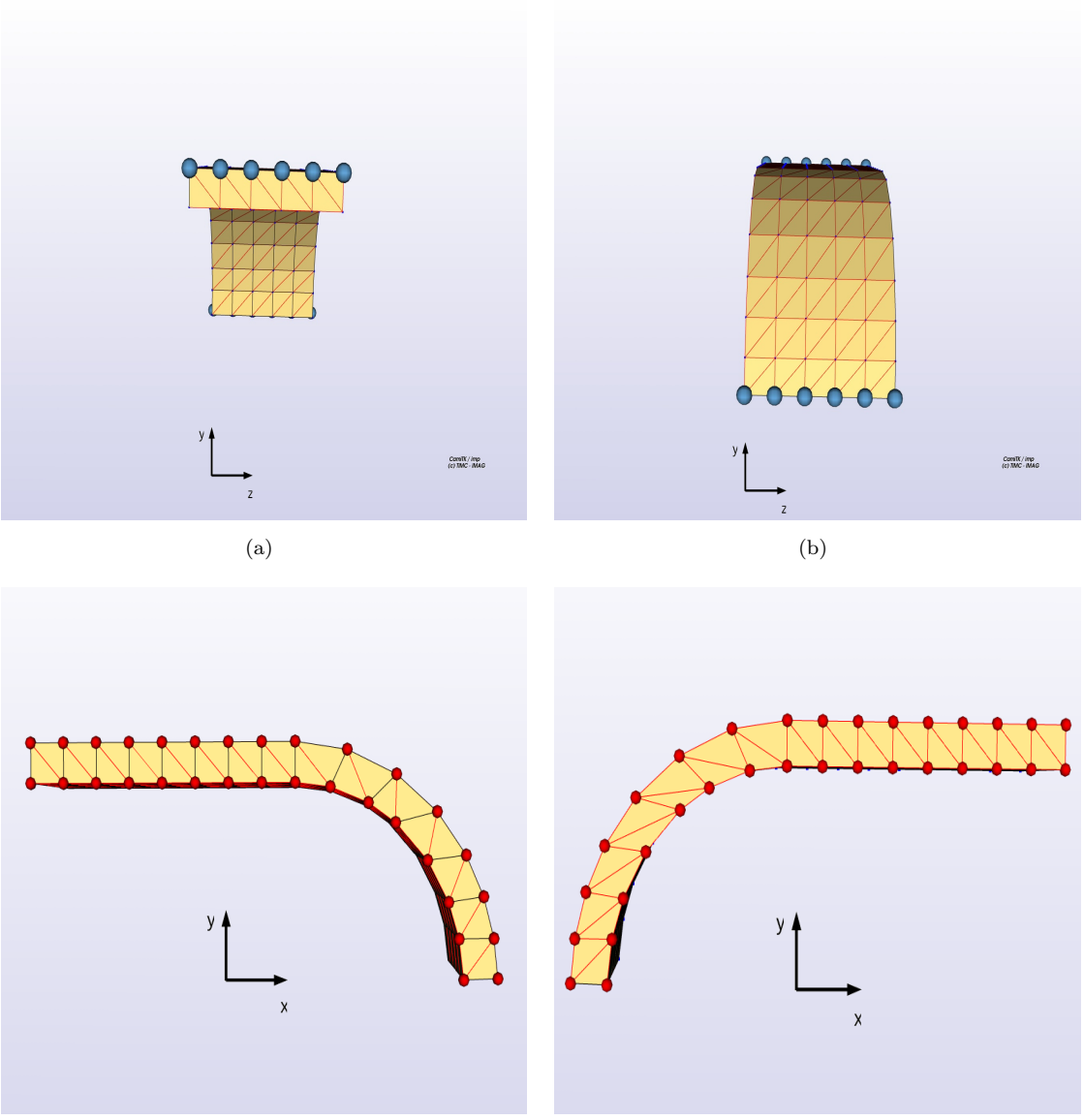

(a) (b)

(c) (d)

FIGURE 2.4: **Representation of the boundary conditions imposed on the structure.** This figure represents the boundary conditions in the undeformed geometry. (a) and (b) The blue sphere denotes the particles that are constrained to a null displacement. (c) and (d) The red sphere denotes the particles whose displacement is restricted to the (x,y) plane. They are the atoms located on the side boundaries of the structure.

Chapter 3

Simulation

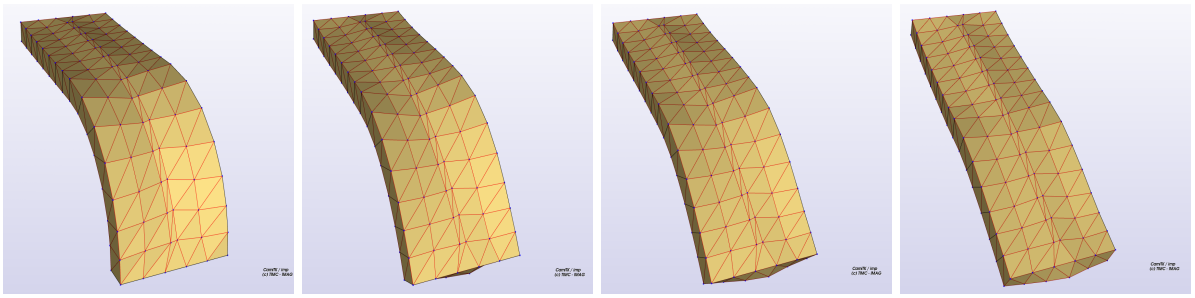

(a)

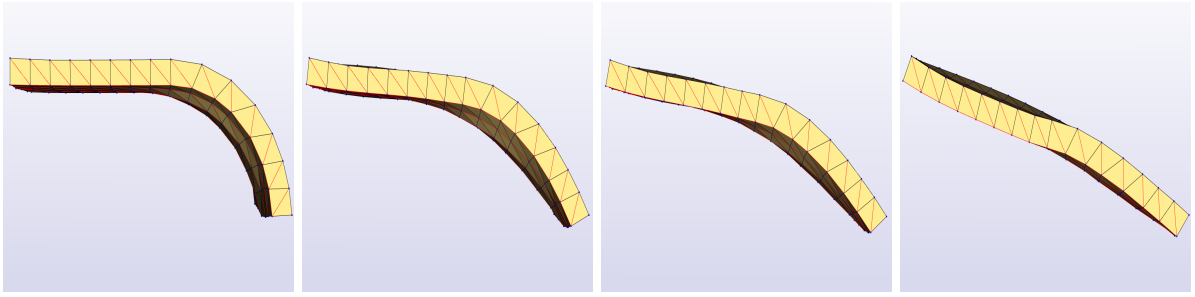

(b)

FIGURE 3.1: **Simulation of the invagination process in the drosophila melanogaster.** Simulation time-steps of the geometry from the top (a) and side (b) for steps #80, #500, #1350, #9120. Note the contracted centered row of cells.

The simulation is divided in time-steps. At each time-step, the following procedures take place:

- The forces are summed up on all the particles and integrated along the structure using a classic integration scheme.
- The velocity and position of each particle are calculated and integrated also along the structure.
- The constraints are applied (incompressibility, boundary consditions)

At the beginning of the simulation, all the particles are submited to forces of equal value. This is acheived by applying uniform elasticity and contractility coefficients along the structure (see section Materials and Methods).

In Figure 3.1, we present the geometry obtained during the simulation for various time-steps, from two different angles. In the first row, the geometry is shown from the top and in the second row, it is shown from the side of the structure.

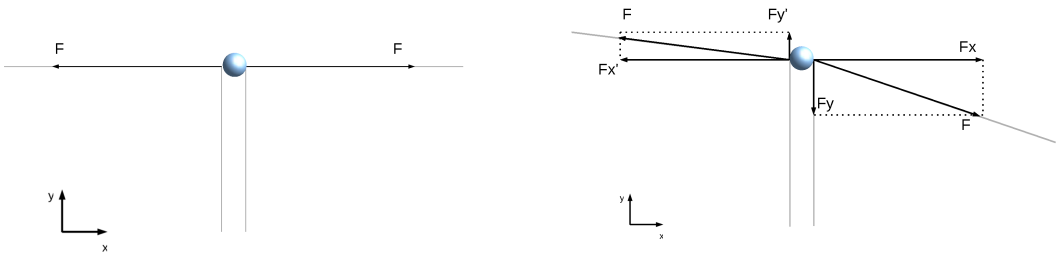

(a) (b)

FIGURE 3.2: **2D representation of the forces on a single particle at the beginning of the simulation** (a) The particle is located at the flat area of our structure. In the beginning, the x and y components of the forces imposed to it are equal, so it only moves on the z axis. (b) The particle is located on the area where the curvature is highest. The value F of the force imposed to it by the next particle is equal to the value F' of the force imposed to it by the previous one. Nevertheless, because of the geometry of the structure, the F_y component is stronger than the F'_y component, so the particle is pulled in a downwards direction. In addition, the F'_x component is stronger than the F_x, resulting to the particle being pulled towards the linear area

At the beginning the cells of the center row are contracting due to the activation of the myosine fibers. This contraction "pulls" all the cells of the model towards the center. Due to the initial geometry of the structure, as shown in Figure 2.2(a), the F_y component of the force F applied on the particles on the curved area, causes the particles to move downward. As the cells located on the center row of the curved part, move down, they concurrently pull the other cells of the structure as well, due to the cell-cell bonds described in Figure 2.3(a). As a result, all the cells start to move downwards (see Figure 3.1). In Figure 3.3, we have a 3D representation of the forces applied to two different cells of the structure at time-step #150 of the simulation. The sum of forces on the particle at the curved area, is approximately 3.3 times bigger than the sum of forces on the particle at the flat area. Due to the shape of the structure, even if the initial

intensity of the forces is equal and uniform along the structure, the cells located at the curved area are pulled downward much quicker than the cells at the flat area.

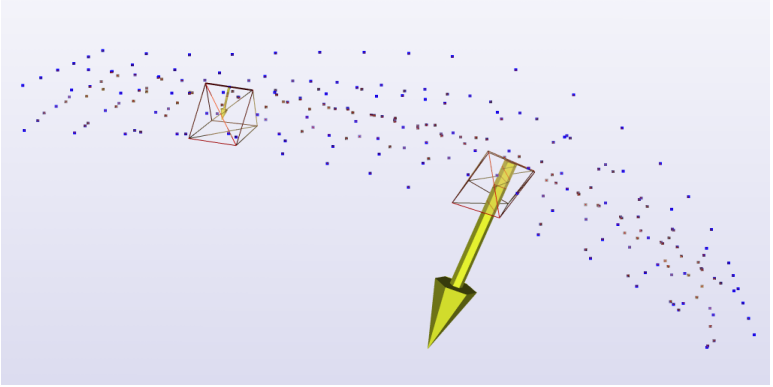

FIGURE 3.3: **Representation of the sum of forces imposed on the center particles of two cells during the course of the simulation.** (a) The force on the cell located at the curved area is much stronger than the force on the cell at the flat area.

An important factor concerning the invagination process is the $surface/volume$ ratio. In vivo experiments have shown that, as the phenomenon advances, the surface of the cell closest to the nourishment factor decreases ([Lep99]). On the other hand, the volume of the cell increases as it gets close to the factor of chemotaxis and nourishes. As a result, the $surface/volume$ ratio decreases as time passes. It has been noted that it can decrease up to a certain threshold, because after that, the cell tends to divide.

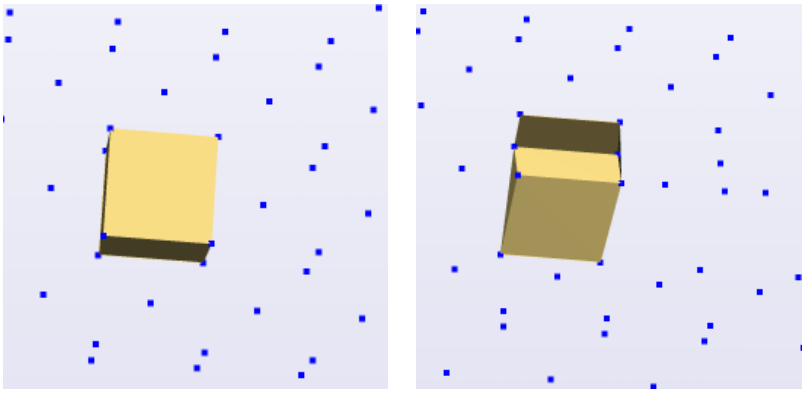

(a) (b)

FIGURE 3.4: **Individual cell shape deformation.** The shape of the cells changes, from an initial regular hexahedral shape (a) to a prismatic shape (b). The surface of the top facet decreases rapidly and at the same time, the surface of the bottom facet increases, resulting to constant volume.

The monitoring of the $surface/volume$ ratio for our model is presented in Figure 3.5(a). Its value is decreasing very rapidly at the beginning of the process, from the value of 0.1 at time-step #1, until it reaches the value of 0.0275 at time-step #59. After that, it continues to decrease slightly and can be considered constant.

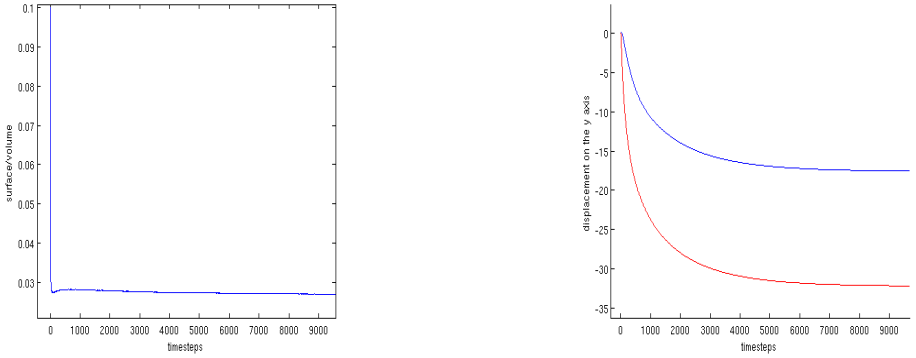

(a) (b)

FIGURE 3.5: **Surface/volume ratio and movement on the y axis of the center particles (centrioles).** (a) The surface to volume ratio decreases exponentially at the beginning of the simulation from 0.1 to 0.0275 at time-step #59. After that, it can be considered constant. (b) The displacement of the center particle of a cell located at the flat area of the structure (blue) is substancially larger and faster than the displacement of the center particle of a cell located at the curved area (red).

In Figure 3.5(b) we monitor the displacement on the y axis of the center nodes of two cells located in the middle row, one at the curved area of the structure and the other at the flat part, normalized in order to start from the same initial point. The cell at the curved area starts to move downward faster than the other cell. At the beginning and up to time-step #47 the velocity on the y axis of the cell at the curved area (red line) is 20 times bigger than the velocity of the cell at the flat area (blue line). At step #250 the velocity of the cell at the curved area is 2 times bigger than the velocity of the cell at the flat area, because the propagation of the bending along the curve has reached the second particle.

Chapter 4

Materials and Methods

4.1 Organization and Geometry

The model implemented is built according to an object oriented approach. This permits us to organize precisely the different concepts and the relations binding them. Each object modeled can be analyzed to other objects with different properties. There are 4 existing types: elastic, muscular, rigid and cellular. The objects of the same type are grouped in the same class. Thus, each object is a particular instance of a certain class but, at the same time, has a unique behavior. Moreover, the object oriented approach permits to organize the classes in a hierarchical way depending on the properties modeled. The laws defining the behavior of an object, are described in each class. They can equally depend on interactions with the environment of the object and on intrinsic properties (mainly mechanic properties as elasticity, ability to contract and incompressibility). In addition, they can change as time passes or be specified by more general laws described in other classes. For example, a muscular cell is considered as an elastic cell in which we have added contraction properties. In Figure 4.1, we present the hierarchical diagram of the classes implemented in the Phymul library.

4.2 Description of the objects

The various objects used during the course of this thesis were described with the aid of the PML language (Physical Markup Language) ([CP04]). This language, which is built based on the format of an XML (eXtensible Markup Language) document, was selected because it allows to create both continuous and discrete-time physical models. It refers to an object-oriented library originally developed by Emmanuel Promayon and enhanced by M. Marchal and A. Carra, during their PhD thesis. We use 2 types of structure in order to describe the geometry of the

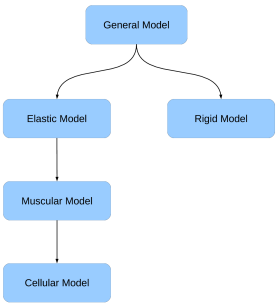

FIGURE 4.1: **The hierarchy of the classes in the phymul library.** The cells in our model have been modeled as cellular objects, which inherit the properties of muscular and elastic objects.

models: particles and cells. The different structures are grouped in components. A structural component engulfs a group of structures (cells or particles) and a multiple component engulfs a group of structural components. A PML document is composed of three main components:

- A list of atoms, defined in a structural component
- A multiple component called exclusive component. There are many structural components included here, but three are the most essential: The description of the different objects which form the model (regions), the description of the neighboring particles of each node (neighborhoods) and the triangular surface for the volume control (enclosed volumes).
- A multiple component called informative component This component is optional and is mainly used for graphic and monitoring reasons

Loads and constraints: In order to implement the constraints to our PML document, we have made extensive use of another XML language, called LML (Loads Markup Language). In an LML document, a load or constraint is defined by the following elements:

- A target with the indices of the structure or the component asked for
- The type of constraint we want to impose (translation, force)
- The direction of the load formed as a 3D vector
- A list of numbers specifying the intensity of the load and the time interval of its application
- The load unit

4.3 Cellular object

As noted in the Organization and Geometry Section, the phymul library gives us the chance to model the objects in 4 different yet dependent ways: rigid, elastic, muscular and cellular. In the context of this project, all cells have been modeled as objects of cellular type, attributed certain characteristics: elasticity, incompressibility and contractility. A cellular object is a deformable object, which keeps its volume stable when forces are applied to it, causing it to deform. Moreover, using muscular forces, we can force the cellular object to contract according to the demands of our experiment. Finally, the elasticity forces connecting its particles, act as shape memory forces.

In the following paragraphs, we are going to describe each one of the properties above and explain their implementation.

Elasticity

The general principle, which we are going to describe here, is that the existence of the elasticity relies on a shape memory force of the formation of the object and on the notion of a virtual attractor.

Let P be the position of a given particle and N, $i \in [1, ..., n]$ the positions of of the n neighbors of this particle. The idea is to express the position P^* of the attractor of the particle as a function of his n neighbors. The neighboring particles are divided into triplets forming triangles (triplets forming straight lines are rejected), with each particle participating in more than one triplets concurrently. All the possible combinations of three particles are taken into account and the norm of each triangle formed by N_i, N_j, N_k, i, j, $k \in [1, ..., n]$ is noted as n_Δ. The position P_Δ of the particle relatively to the triplet $\langle\ N_i,\ N_j,\ N_k\ \rangle$ is given by the following statement:

$$P_\Delta = Q_\Delta + \beta_\Delta \frac{n_\Delta}{\parallel n_\Delta \parallel} \tag{4.1}$$

where Q_Δ is the projection of P on $\langle\ N_i,\ N_j,\ N_k\ \rangle$ according to the n_Δ norm and β_Δ is the distance between P_Δ and Q_Δ. As a result, P^* is defined as the isobarycenter of all the P_Δ positions, resulting from the valid triplet formed by all the neighbors of the considered particle.

$$P^* = \frac{1}{m} \sum_{\Delta=1}^{m} (Q_\Delta + \beta_\Delta \frac{n_\Delta}{\parallel n_\Delta \parallel}) \tag{4.2}$$

If one or more neighbors of the given particle moves, the position of the attractor of the particle is going to change. Consequently, a memory force F^* is generated between the current position of the particle and the position of its attractor, given by the following statement:

$$F^* = k_e(P^* - P) \tag{4.3}$$

where k_e is the elasticity coefficient (which in our project is defined as a simple scalar uniformly distributed along the structure). Finally, the memory force is redistributed to all the neighboring particles which participated in the calculation of the attractor.

Contractility

The muscular objects are a particular case of elastic objects. The characteristics of a muscle are its anatomical attachments, its mechanic and electric properties and, mainly, the fibers which it incorporates. An attractor is built in the fibers of the object to induce this contracting behavior to an elastic tissue. The principle used here is that of a force created by an attractor. The directions of the force are defined locally for each particle. Each neighboring particle located in the direction of the contraction is regarded as an attractor. An internal force F^* is generated between the current position P of a particle and the position P^* of each of its attractors. It is stated as:

$$F^* = k_m(P_i^* - P) \tag{4.4}$$

where k_m is the muscular coefficient. Like the elasticity coefficient, it is equally distributed along the structure. This coefficient models the activation, contraction and relaxation phases. It can vary as time passes and from one particle to another. A positive coefficient yields to an active contraction. When k_m has decreased to zero, the cell returns to each original configuration, due to the elasticity property. The muscular force generated by a given particle on one of its neighbors is automatically redistributed to the latter (by inverting the sign of the force vector).

Incompressibility

In this section, we present the main points of the method implemented to control the volume. Consider the surface of an object in 3D represented by a polyhedron with n vertices. Let P_1,...,P_n be the positions of these vertices and F_1,..., F_m the m facets of the surface of the structure. We note as X the vector of size $3n$ composed by the positions of all the vertices: X=(P_1,...,P_n), which is the vector describing the state of the polyhedron. In addition, we note

as $V(X)$ the function of the volume of the polyhedron with V_0 its initial volume. The technique implemented is as follows: Suppose there is a deformation of the polyhedron represented by the vector X^*. The method implemented allows us to find a vector X' similar to X^*, whose volume is equal to V_0 (the initial volume). Consequently, what we need to do is to determine the displacement of each vertex, solving the following system:

$$\begin{cases} X' = X^* + \lambda \nabla V(X^*) \\ V(X') = V_0 \end{cases} \tag{4.5}$$

where $\nabla V(X)$ is the gradient of the volume function $V(X)$ and λ is a scalar.

Considering the vertices of the polyhedron, the system 4.5 can be written as:

$$\begin{cases} P_i' = P_i^* + \lambda \nabla_i, \forall i \in [1, ..., n] \\ V(X') = V_0 \end{cases} \tag{4.6}$$

where ∇_i is the part of $\nabla V(X^*)$ concerning P_i:

$$\nabla_i = \frac{\partial \nabla V(P_i^*)}{\partial P_i^*} \tag{4.7}$$

The calculation of the volume of the polyhedron is based on the isobarycenter of each of the m facets. It derives from the following equation:

$$V(X) = \frac{1}{3} \sum_{j=1}^{m} G_j A_j \tag{4.8}$$

where G_j and A_j represent respectively the barycenter and the surface vector of the j^th facet.

If we consider the vector S_i containing all the facets of the polyhedron including the vertex P_i, the volume can be expressed as:

$$V(X) = \frac{1}{3N} \sum_{j=1}^{n} P_i \left(\sum_{F_j \in S_i} \frac{A_j}{n_j} \right) \tag{4.9}$$

and in the case where all the facets of the polyhedron have the same number of vertices N, we have:

$$V(X) = \frac{1}{3N} \sum_{i=1}^{n} P_i A_i \tag{4.10}$$

This allows us to determine for every vertex P_i its part V_i in the total volume $V(X)$:

$$V_i = \frac{1}{3N} P_i A_i \tag{4.11}$$

With the aid of 4.11, the final solution can derive from the following system of equations:

$$\begin{cases} P_i' = P_i^* + \lambda \nabla_i, \forall i \in [1, ..., n] \\ \sum_i = V_i' = V_0 \end{cases} \tag{4.12}$$

with

$$\nabla_i = \frac{1}{3N} A_i \tag{4.13}$$

where P_i' is a vector denoting the new position of each particle, ∇_i is the i-th gradient of the volume function $V(X)$ and A_i is the area vector of the i-th facet.

Since every facet of the polyhedron is a triangle ($N = 3$), the solution of the previous system is given by a third degree equation where λ is unknown. Then, the displacements on the vertices of the polyhedron are applied according to the value of λ.

Chapter 5

Conclusions and discussion

5.1 Conclusions

Our simulation, came up with two very important results:

- The change of the shape of the structure starts at the area where the curvature is higher and, as time passes, it propagates to the linear area. This is precisely the behavior of cells noticed in the in vivo experiments, as pointed in [MKW08].
- Although the distribution of forces is equal along the whole structure, only its geometry can explain that the first cells to be affected are the ones at the curved area. This is due to the force component pulling the particles downward, as shown in Figure 3.2(b).

Consequently, we have created a model exclusively based on physics and geometry, which we consider to be efficiently simulating the beginning of the process of invagination.

5.2 Discussion and further work

The intention of this scientific work is to provide first proof supporting the assumption that, gastrulation, a very important early stage of morphogenesis, is a procedure controlled merely by physics. To accomplish that, all types of mass cellular movements taking place during gastrulation need to be modeled and simulated: ingression, invagination, involution, epiboly, intercalation and convergent extension. Models simulating effectively all these processes have been created (see [OOBA80], [DF00], [LG90], [CNP$^+$08]) but none of them rely exclusively on the laws of physics and geometry.

In our project, we have modeled the area of the cellular aggregate where the phenomenon of invagination begins. Although the simulation verified our original hypothesis, the model is not complete. In order to have definitive results, the whole tube must be modeled. By running simulations on this new structure and receiving the same feedback, we can positively say that the initiation of the invagination is a process which can be described by relying exclusively on the laws of physics and mechanics.

We made an assumption regarding the bonds between cells. As mentioned previously, the cells are strongly adherent to each other due to the use of cadherins. We have considered here that cadherins are located on the vertices of the touching sides of neighboring cells, as shown on Figure 2.3(a), based on [DCEM09]. Nevertheless, not all scientific representations of cadherins agree that they are located on specific points of the cells. In fact, their number is so big, that they could be considered to be everywhere on the surface of the cell. Consequently, more simulations have to be made, supporting other suppositions about the location of the connecting liaisons of neighboring cells, for example with adherence focal points located on the geometrical center of the frontiers of the cells, as shown in Figure 2.3(b).

In [Lep99], it is suggested that, at the beginning of invagination, the centriole moves towards the opposite side of the contracting area and approaches the bending of the structure, while, at the end, it is relocated to the nucleus of the cell. In our simulation, the displacement of the centriole of each cell is passive and does not comply with the movement suggested in [Lep99]. We have not set any specific regulation so it moves according to the displacement of the entire cell. At the beginning it stays still and, as the cell begins to move downwards, the centriole follows this movement. At the end, it stays attached to the contracting facet. We consider that if the displacement of the centrioles is efficiently explained and modeled, it will be a very crucial step towards understanding the behavior of cells during gastrulation. The centriole is the most important part of the microtubule-organizing center of the cell, the centrosome ([FGM07]).

Finally, during the invagination process, cells whose volume increases further than a certain limit, tend to divide. Figure 3.5(a) clearly shows that our simulation should take into account the division process. The sudden decrease of the surface/volume ratio for real cells triggers cell division, which results to the further deepening of the curve. Our model cannot form a bending deep enough, as experiments in vivo suggest, unless the cell division process is included in the simulation.

Bibliography

[ADG09] L. Abbas, J. Demongeot, and N. Glade. Synchrony in reactionb•"diffusion models of morphogenesis: applications to curvature-dependent proliferation and zero-diffusion front waves. *PTRS A*, 367(1908), 2009.

[ASK98] H. Aberle, H. Schwartz, and R. Kemler. Cadherin-catenin complex: Protein interactions and their implications for cadherin function. *Journal of Cellular Biochemistry*, 61(4):514–523, 1998.

[CNP+08] M. Coolen, D. Nicolle, J.L. Plouhinec, A. Gombault, T. Sauka-Spengler, A. Menuet, C. Pieau, and S. Mazan. Molecular characterization of the gastrula in the turtle emys orbicularis: An evolutionary perspective on gastrulation. *PLoS ONE*, 3(7), 2008.

[CP04] M. Chabanas and E. Promayon. Physical model language: Towards a unified representation for continuous and discrete models. *Lecture Notes in Computer Science*, 3078:256–266, 2004.

[DCEM09] I. Dupin, E. Camand, and S. Etienne-Manneville. Classical cadherins control nucleus and centrosome position and cell polarity. *JCB*, 185:5779–5786, 2009.

[DF00] D. Drasdo and Gabor Forgacs. Modeling the interplay of generic and genetic mechanisms in cleavage, blastulation, and gastrulation. *Developmental Dynamics*, 219:182–191, 2000.

[DHPC+05] R.E. Dawes-Hoang, K.M. Parmar, A.E. Christiansen, C.B. Phelps, A.H. Brand, and E.F. Wieschaus. folded gastrulation, cell shape change and the control of myosin localization. *Development*, 132:4165–4178, 2005.

[FD08] L. Forest and J. Demongeot. A general formalism for tissue morphogenesis based on cellular dynamics and control system interactions. *Acta Biotheoretica*, 56(1-2):51–74, 2008.

[FGM07] J.L. Feldman, S. Geimer, and W.F. Marshal. The mother centriole plays an instructive role in defining cell geometry. *PLoS Biol*, 5(6), 2007.

[HK88] J. Hardin and Ray Keller. The behaviour and function of bottle cells during gastrulation of xenopus laevis. *Development*, 103:211–230, 1988.

[Lep99] M. Leptin. Gastrulation in drosophila: the logic and the cellular mechanisms. *EMBO J*, 18(12):3187b•“3192, 1999.

[LG90] M. Leptin and B. Grunewald. Cell shape changes during gastrulation in drosophila. *Development*, 110:73–84, 1990.

[MKW08] A.C. Martin, M. Kaschube, and E.F. Wieschaus. Pulsed contractions of an actin-myosin network drive apical constriction. *Nature*, 457:495–499, 2008.

[OOBA80] G. Odell, G. Oster, B. Burnside, and P. Alberch. A mechanical model for epithelial morphogenesis. *Journal of Mathematical Biology*, 9(3):291–295, 1980.

[Tak91] M. Takeichi. Cadherin cell adhesion receptors as a morphogenetic regulator. *Science*, 251(5000):1451 – 1455, 1991.